ELSEVIER

Biochimica et Biophysica Acta 1232 (1995) 175–179

BBA Biochimica et Biophysica Acta

The geometry and spin density distribution of the tyrosyl radical: a molecular orbital study

Patrick J. O'Malley [a,*], Andrew J. MacFarlane [a], Stephen E.J. Rigby [b], Jonathan H.A. Nugent [b]

[a] *Department of Chemistry, UMIST, Manchester, M60 1QD, UK*
[b] *Department of Biology, University College, London, WC1E 6BT, UK*

Received 6 April 1995; accepted 23 June 1995

Abstract

The oxidation of the amino acid tyrosine to the tyrosyl radical is now known to be important in many electron transfer reactions in biology. Electron Paramagnetic Resonance (EPR) and Electron Nuclear Double Resonance (ENDOR) have previously been used to obtain proton hyperfine couplings for the radical in vivo. This study uses AM1 molecular orbital calculations to provide a detailed insight into the geometry and electronic makeup of this important radical. Molecular orbital studies are first used to obtain an optimised geometry for the tyrosyl radical. This is shown to differ significantly from the unoxidised form. The extent of the singly occupied molecular orbital is then examined and a theoretical estimate of the unpaired electron spin distribution is obtained. This is then used to calculate the anisoptopic hyperfine coupling components for comparison with experimental determinations.

Keywords: Molecular orbital; Tyrosine; Geometry; Spin density distribution; EPR; ENDOR

1. Introduction

Electron transfer agents in biology are generally thought to be associated with metal centres or cofactors such as quinones or flavins. Only very recently has the important role played by oxidisable amino acid residues been appreciated [1]. This role is apparently played by the amino acids tyrosine, tryptophan and possibly histidine.

Tyrosine has now been shown to be involved in electron transfer events in Photosystem II [2], ribonucleotide reductase [3], prostaglandin synthase [4], galactose oxidase [5] and amine oxidase [6]. Electron paramagnetic resonance (EPR) has been widely used to study the radical species involved. Proton hyperfine interactions with the distribution of the unpaired electron spin density gives rise to a broadened EPR spectrum whose spectral features can vary considerably depending on the species studied. The EPR spectrum is dominated by the larger electron-nuclear hyperfine interactions and it is the variation in these from species to species that results in the differing EPR spectral characteristics [1].

ENDOR spectroscopy can be used to obtain directly the individual hyperfine coupling values. The utility of ENDOR is most easily appreciated in liquid state studies where resonances due to hyperfine interactions occur at the isotropic coupling values. In the absence of single crystal data, most biological studies have to utilise powder ENDOR spectroscopy where contributions from all possible orientations result in a considerable broadening of spectral lines. The demonstration that a build up of intensity occurs at the principal hyperfine tensor values for the electron nuclear hyperfine interaction [7] suggested the feasibility of recovering this information from the powder ENDOR spectrum. In the absence of specific deuteration studies the assignment of spectral resonances is difficult and any assignments need to be supported by theoretical predictions from molecular orbital studies. The ENDOR spectrum of the stable tyrosyl radical in Photosystem II has

Abbreviations: EPR, Electron Paramagnetic Resonance; ENDOR, Electron Nuclear Double Resonance; HOMO, Highest Occupied Molecular Orbital; SOMO, Singly Occupied Molecular Orbital; AM1, Austin Method 1; INDO, Intermediate Neglect of Differential Overlap.

* Corresponding author. Fax: +44 161 2367677 or 6; e-mail: patrick@trigger.ch.umist.ac.uk.

SSDI 0005-2728(95)00102-6

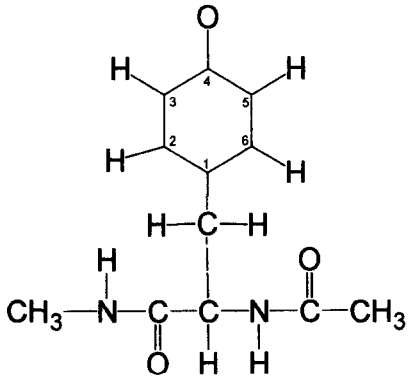

Fig. 1. *N*-Acetyltyrosylmethylamide radical plus numbering scheme used for the molecular orbital calculations.

been recently obtained by us [13] and assignments of the spectral lines has been made by a combination of (1) comparison with other similar radicals, (2) difference spectra, (3) orientation selection, and (4) EPR spectral simulation.

In previous studies on the tyrosyl radical we have calculated the isotropic coupling constants using a combination of AM1 and INDO [8]. Here we use the AM1 method to study the geometry of the radical and combine this with the unpaired spin density distribution to calculate the anisotropic couplings. Many studies have been carried out on the geometry of the related phenoxyl radical [9,10]. This area is well summarised in a recent publication [10]. Despite the complete failure of many high level Hartree-Fock level calculations to predict the geometry of this radical, there is excellent agreement between the AM1 predicted geometry and the best CAS-SCF/6-311G(2d,p) result [10]. For this reason and due to the size of the molecule considered here we have chosen the AM1 method to provide us with a geometry and spin density distribution for the tyrosyl radical.

The AM1 molecular orbital studies are used to obtain an optimised geometry and first order spin density distribution for the tyrosyl radical. From this geometry and spin density distribution the theoretical anisotropic hyperfine couplings are calculated and compared with the experimental ENDOR data. In this way the geometry of the tyrosyl radical is obtained and a firm theoretical basis for the assignment of the experimentally observed resonances to electron nuclear hyperfine interactions is developed.

2. Methods

The unit tyrosine derivative used for the molecular orbital calculations is shown in Fig. 1. The numbering system used is also given. The molecular orbital calculations were performed with the AM1 [12] method using the MOPAC programme running on a Silcon Graphics workstation.

3. Results and discussion

In previous studies it has been assumed that the geometry of the tyrosyl radical is identical to the unoxidised amino acid [11]. Radical generation with associated deprotonation can be expected to alter the geometry of the molecule and therefore we have used molecular orbital calculations to optimise the geometry of the tyrosyl radical. The calculations were performed at the semiempirical AM1 level of theory [12] and the procedure used is described in the methods section. To test the accuracy of the calculated geometry we have also performed a geometry optimisation of the unoxidised tyrosine at the same level of theory. This result can then be compared with that obtained from neutron diffraction data for tyrosine [14]. Fig. 2 compares the calculated and experimental geometries in terms of both bond lengths and bond angles. The agreement between the theoretical and experimental values is excellent showing the good predictability of this level of theory. The calculated bond lengths and bond angles for the tyrosyl radical are shown in Fig. 3. Significant differences between the radical geometry and the unoxidised tyrosine are noted. Bonds C2-C3, C5-C6 and C4-O become shorter, while C1-C2, C3-C4, C4-C5 and C6-C1 become longer. Small changes in the bond angles also accompany these bond length changes. These results indicate that the original aromatic ring system adopts a quinoid-like structure on radical formation, with bonds

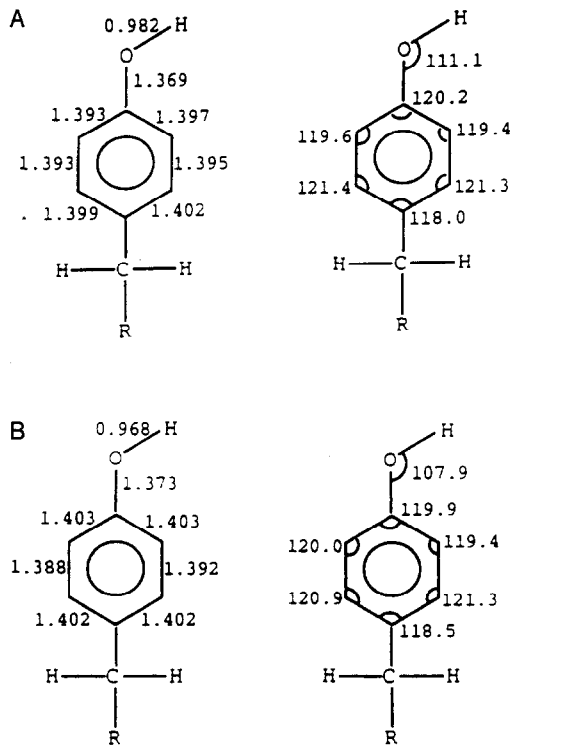

Fig. 2. (a) Geometry obtained from neutron diffraction studies of tyrosine according to Ref. [14]. (b) Geometry obtained after geometry optimisation at the AM1 level.

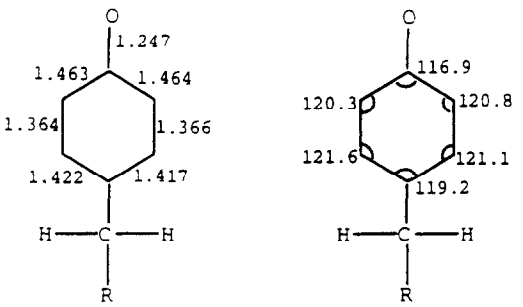

Fig. 3. Geometry of the tyrosyl radical after geometry optimisation at the ROHF AM1 level.

C2-C3 and C5-C6 being shorter than the other carbon-carbon bonds in the ring system and the carbon-oxygen bond also contracting in length. On closer examination of the bond lengths it is observed that the C1-C2 and C6-C1 bonds are shorter than the C3-C4 and C4-C5 bonds. This suggests more delocalisation in the lower part of the ring compared with the upper part. One explanation for these geometrical features can be found by examining the classical resonance structures for the tyrosyl radical, Fig. 4. In these resonance forms there is the greatest amount of double bond character for C4-O, C2-C3 and C5-C6 and the least for C3-C4 and C4-C5.

The geometrical changes on oxidation also reflect the variation in the extent of the highest occupied molecular orbital for both unoxidised and oxidised species. A sketch of the HOMO for the unoxidised form is compared with the singly occupied molecular orbital (SOMO) for the oxidised form in Fig. 5. The lengthening of the C1-C2, C6-C1, C3-C4 and C4-C5 bonds on oxidation can be qualitatively explained by the decreased electron density between these bonds in the oxidised form. The form of the SOMO for the radical species also gives us a qualitative picture of the distribution of the unpaired electron around the radical. Unpaired electron spin density is expected to predominate at carbon positions C1, C3, C5 and at the oxygen atom. The unpaired electron spin density values at each position around the ring system are given in Fig. 6a. It is now possible to compare this spin density distribution with that estimated from experimental EPR and ENDOR measurements [13].

From experimental ENDOR studies, the unpaired electron spin density distribution shown in Fig. 6b has been obtained. Good agreement is indicated for most positions except ring carbons C2 and C6. The experimental data indicate, however, significant hyperfine coupling between the spin density at C2, C6 and the attached protons. The appearance of unpaired spin at what is predicted from theory to be a nodal position is due to a slight unpairing of the electron density of the formally paired electrons by the presence of an unpaired electron in the singly occupied orbital [15]. Restricted Hartree Fock theory does not allow for this and hence predicts zero spin density for carbon atoms C2 and C6. Unrestricted Hartree Fock theory can allow for this effect, but attempts to perform calculations at this level led to a high degree of spin contamination from states other than the pure doublet. A direct measure of this spin density value can be obtained from the liquid solution EPR studies of the tyrosyl radical [16,17]. A value of 4.3 MHz is observed. This corresponds to a C(2,6)π orbital spin density of -0.06 (McConnell Q value of -69.6 MHz [13]). Adopting this value of -0.06 for the C2 and C6 positions and raising the spin density value on the neighbouring carbon atoms by 0.03, we arrive with the spin density distribution of Fig. 6c. This spin density distribution is in good agreement with the distribution proposed by Rigby et al. [13] for the Photosystem II radical. A test of the accuracy of this spin density distribution can be obtained by calculating the anisotropic components for the interactions and comparing with experimental determinations.

A detailed ENDOR study of the stable tyrosyl radical in Photosystem II has recently been carried out in our laboratories [13]. The principal values of the hyperfine tensors have been obtained and can be used for comparison with our theoretical values. Using the method originally developed by McConnell and Strathdee [18], it is possible to calculate the principal values for the anisotropic coupling tensors given the π spin density distribution and the geometry of the radical. A previous study on the tyrosyl

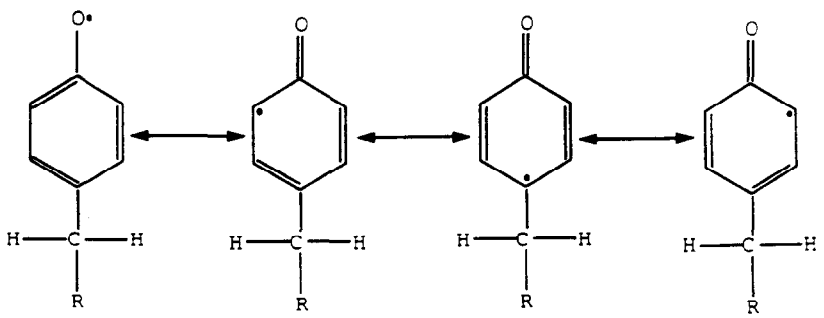

Fig. 4. Classical resonance structures for the tyrosyl radical.

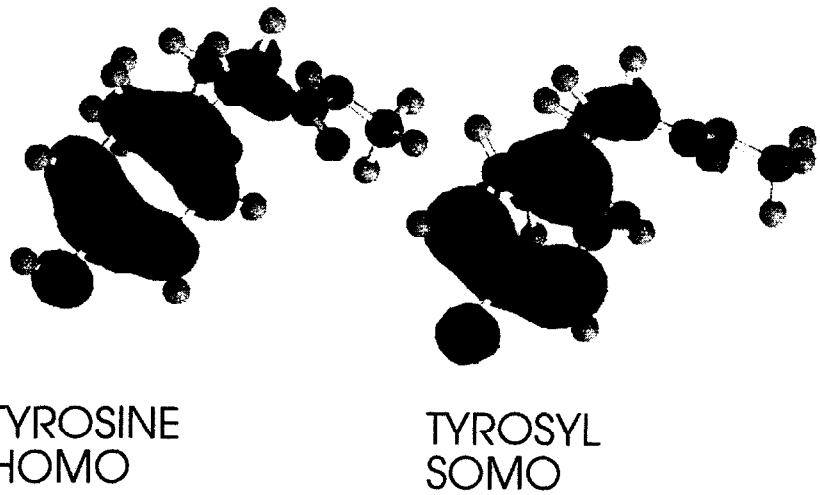

Fig. 5. (a) Highest occupied molecular orbital(HOMO) for tyrosine. (b) Singly occupied molecular orbital(SOMO) for the tyrosyl radical.

radical in ribonucleotide reductase [11] used the McConnell and Strathdee method in its original formalism and utilised the unoxidised geometry. However, the method has been substantially improved by Falle et al. [19,20]. The principal change is the inclusion of a term for the calculation of the effective nuclear charge (E_π) having the form:

$$E_\pi = 1.2969 + 0.24182\rho_\pi^2$$

thereby making it dependent on the atomic spin density value(ρ_π).

The spin density distribution used was that given in Fig. 6c and the geometry used was that given in Fig. 3. The detailed procedure used in the calculation of the tensors has been described [21]. For the ring protons the following principal values are calculated (MHz):

*H*6	A_x 4.8	A_y 7.7	A_z 0.1
	(4.4)	(7.2)	(−)
*H*2	A_x 4.9	A_y 7.7	A_z 0.0
	(4.6)	(7.4)	(−)
*H*3	A_x −26.4	A_y −8.3	A_z −19.6
	(−25.6)	(−8.0)	(−19.1)
*H*5	A_x −27.4	A_y −8.6	A_z −20.3
	(−27.5)	(−8.0)	(−20.5)

In brackets are given the values deduced from ENDOR spectroscopy by Rigby et al. [13] for the dark stable tyrosyl radical of photosystem II. Good agreement is also found with the experimental values determined for the ribonucleotide reductase radical [11]. The calculated values described here confirm these previous assignments and indicate impressive agreement between calculated and experimental data.

The anisotropic couplings for the β methylene protons have been calculated, using the geometry and spin density distribution described above, according to the method proposed by Derbyshire [22]. Using the isotropic coupling value of the Photosystem II radical [13], the values calculated for the large coupling β proton (experimental values for Photosystem II in brackets) are (MHz):

A_x 33.8	A_y 26.4	A_z 25.6
(31.5)	(27.2)	(27.2)

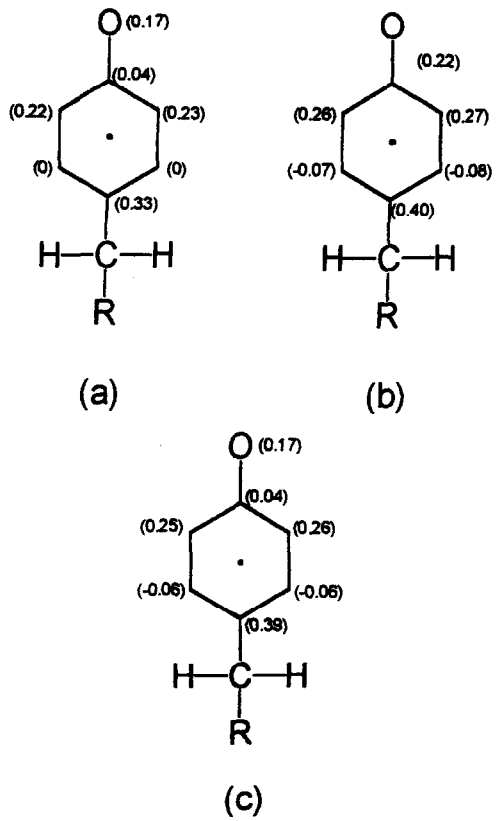

Fig. 6. (a) ROHF AM1 calculated spin density distribution for the tyrosyl radical. (b) Experimentally determined spin density distribution from reference [13] (c) Proposed spin density distribution for the tyrosyl radical.

For the smaller coupling proton the values are (MHz):

A_x 12.2	A_y 2.3	A_z 4.5
(9.8)	(4.6)	(4.6)

While the agreement between experiment and theory is not as good as that observed for the ring proton couplings, the calculated values lend support to the experimental assignments.

4. Conclusions

This study has used the AM1 molecular orbital method to describe in detail the geometry of the tyrosyl radical, its wavefunction and the distribution of unpaired electron spin density in the radical. The molecular orbital calculations indicate that significant geometrical changes accompany oxidation of tyrosine to form the tyrosyl radical. The radical geometry and its ensuing unpaired spin density distribution is used to calculate the anisotropic hyperfine tensor principal values for the proton electron hyperfine interactions. These data support the previous assignments of Rigby et al. [13] and provide a consistent picture of the spin density distribution of this important radical.

References

[1] Prince, R.C. (1988) Trends Biochem. Sci. 13, 287–294.
[2] Prince, R.C. (1990) Trends Biochem. Sci. 15, 170–172.
[3] Sjoberg, B.-M., Reichard, P., Grasslund, A. and Ehrenberg, A. (1978) J. Biol. Chem. 253, 6863–6865.
[4] Smith, W.L., Eling, T.E., Kulmacz, R.J., Marnett, L.J. and Tsai, A.L. (1992) Biochemistry 31, 3–7.
[5] Whitaker, M.M. and Whitaker, J.W. (1990) J. Biol. Chem. 265, 9610–9613.
[6] Jones, S.M., Mu, D., Wemms, D., Smith, A.J., Kaus, S., Maltby, D., Burlingame, A.L. and Kinman, J.P. (1990) Science 248, 981–987.
[7] O'Malley, P.J. and Babcock, G.T. (1984) J. Chem. Phys. 80, 3912–3915; O'Malley, P.J. and Babcock, G.T. (1986) J. Am. Chem. Soc. 108, 3995–4005.
[8] O'Malley, P.J. and MacFarlane, A.J. (1992) J. Mol. Struct. (Theochem.) 277, 293–300.
[9] Armstrong, D.R., Cameron, C., Nonhebel, D.C. and Perkins, P.G. (1983) J. Chem. Soc. Perkin Trans. II, 569–573.
[10] Chipman, D.M., Liu, R., Zhou, X. and Pulay, P. (1994) J. Chem. Phys. 100, 5023–5035.
[11] Bender, C.J., Sahlin, M., Babcock, G.T., Barry, B.A., Chandrashekar, T.K., Salowe, S.P., Stubbe, J., Lindstrom, B., Peterson, L., Ehrenberg, A. and Sjoberg, B.-M. (1989) J. Am. Chem. Soc. 111, 8076–8092.
[12] Dewar, M.J.S., Zoebisch, E.G., Healy, E.F. and Stewart, J.J.P. (1985) J. Am. Chem. Soc. 107, 3902–3910.
[13] Rigby, S.E.J., Nugent, J.H.A. and O'Malley, P.J. (1994) Biochemistry 33, 1734–1742.
[14] Frey, M.N., Koetzle, T.F., Lehmann, M.S. and Hamilton, W.C. (1973) J. Chem. Phys. 58, 2547–2551.
[15] Wertz, J.E. and Bolton, J.R. (1972) Electron Spin Resonance: Elementary Theory and Practical Applications, McGraw-Hill, New York.
[16] Sealy, R.C., Harman, L., West, P.R. and Mason, R.P. (1985) J. Am. Chem. Soc. 107, 3401–3406.
[17] Box, H.C., Budzinski, E.E. and Freund, H.G. (1974) J. Chem. Phys. 61, 2222–2226.
[18] McConnell, H.M. and Strathdee, J. (1959) Mol. Phys. 2, 129–135.
[19] Falle, H.R. and Luckhurst, G.R. (1970) J. Mag. Reson. 3, 161–174.
[20] Falle, H.R. and Whitehead, M.A. (1972) Can. J. Chem. 50, 139–148.
[21] MacFarlane, A.J. (1993) PhD Thesis, University of Manchester.
[22] Derbyshire, W. (1962) Mol. Phys. 5, 225–232.